Anti-Cancer Drugs 2002, **13,** pp. 759–765

Report

15-Deoxy-$\Delta^{12,14}$-prostaglandin J_2 induces apoptosis of a thyroid papillary cancer cell line (CG3 cells) through increasing intracellular iron and oxidative stress

Shu-Yi Chen,[1] Fung-Jou Lu,[1] Rung-Jiun Gau,[1] Mei-Ling Yang[1] and Tien-Shang Huang[2]
[1]Graduated Institute (Department) of Biochemistry and Molecular Biology, and [2]Department of Internal Medicine, College of Medicine, National Taiwan University, National Taiwan University Hospital, Taipei 100-02, Taiwan, ROC.

Treatment of carcinoma cell lines with 15-deoxy-$\Delta^{12,14}$-prostaglandin J_2 (15d-PGJ_2), a natural ligand of the peroxisome proliferator-activated receptor-γ, has been reported to induce apoptosis and/or inhibit proliferation. In this study, we investigated the cytotoxic effect and the action mechanisms of 15d-PGJ_2 in a thyroid papillary cancer cell line, CG3. The results indicate that 15d-PGJ_2 caused cytotoxicity and increased the amount of intracellular reactive oxygen species (ROS) in these cells. Mitochondrial oxidative phosphorylation inhibitors (carbonyl cyanide *m*-chlorophenylhydrazone, oligomycin, cyclosporin A and rotenone), NADPH oxidase inhibitor (diphenyleneiodonium), xanthine oxidase inhibitor (allopurinol) and NO synthase inhibitor (*N*-monomethyl-L-arginine acetate) did not reduce the generation of ROS. However, catalase, *N*-acetyl-cysteine and the iron chelator desferrioxamine decreased the intracellular ROS of 15d-PGJ_2-treated CG3 cells. Furthermore, 15d-PGJ_2 enhanced the accumulation of iron in the CG3 cells. These data suggest that 15d-PGJ_2 induces the generation of ROS by enhancing the accumulation of intracellular iron and that the increased oxidative stress may cause apoptosis of CG3 cells. [© 2002 Lippincott Williams & Wilkins.]

Key words: 15-Deoxy-$\Delta^{12,14}$-prostaglandin J_2, apoptosis, free iron, oxidative stress, thyroid papillary carcinoma.

Introduction

It has been reported that 15-deoxy-$\Delta^{12,14}$-prostaglandin J_2 (15d-PGJ_2), a natural ligand for the peroxisome proliferator-activated receptor (PPAR)-γ,[1] induces apoptosis or inhibits cell growth of many human cancer cell lines, including those from breast,[2] lung,[3] stomach,[4] prostate,[5] thyroid[6] and neuroblastoma.[7] However, the mechanism of 15d-PGJ_2-induced apoptosis is still unclear.

Oxygen is ubiquitous in aerobic organisms, and the generation of reactive oxygen species (ROS) is frequently irresistible and harmful to the cells. The common forms of ROS include superoxide ($O_2^{\cdot -}$), hydroxyl radicals ($OH^{\cdot}$), hydrogen peroxide (H_2O_2), and nitric oxide ($NO^{\cdot}$). ROS may come from different sources, including mitochondrial oxidative phosphorylation,[8] ionizing radiation,[9] inflammation[10] and endogenous enzyme systems, e.g. plasma membrane NADPH oxidase and cytoplasmic xanthine oxidase.[11] ROS can damage various cellular constituents, including DNA, RNA, proteins, lipids, carbohydrates, etc. However, intracellular antioxidants (reduced glutathione and thioredoxin) and antioxidative enzymes [catalase (Cat), superoxide dismutase and glutathione peroxidase] can prevent tissue oxidative damage under normal conditions.[12] Many studies have demonstrated that ROS can induce apoptosis in various cell systems.[13] There are also examples of inhibition of apoptosis by anti-oxidative drugs or enzymes.[14]

In the present study, we observe that 15d-PGJ_2 induces apoptosis of a thyroid papillary cancer cell line, CG3, through the generation of intracellular ROS. It also demonstrated that the generation of ROS resulted from the accumulation of intracellular iron.

This study is supported by a grant from National Taiwan University Hospital (89S1015).

Correspondence to T-S Huang, Department of Internal Medicine, National Taiwan University Hospital, 7 Chung-Shan South Road, Taipei 100-02, Taiwan, ROC.
Tel: (+886) 2 23123456; Fax: (+886) 2 23916956;
E-mail: huang@ha.mc.ntu.edu.tw

Materials and methods

Reagents

15d-PGJ_2 was obtained from Calbiochem Novabiochem (San Diego, CA). Carbonyl cyanide *m*-chloro-

phenylhydrazone (CCCP) was purchased from Ana-Spec (San Jose, CA). Oligomycin (Oli), cyclosporin A (Cys A), rotenone (Rot), diphenyleneiodonium (DPI), allopurinol (All), Cat, *N*-acetylcysteine (NAC), desferrioxamine (DFO), propidium iodide (PI) and luminol were obtained from Sigma (St Louis, MO). *N*-Monomethyl-L-arginine acetate (L-NMMA) was purchased from RBI (Natick, MA). 2,7-Dichlorodihydrofluorescein diacetate (DCFH-DA) and calcein-AM were purchased from Molecular Probes (Eugene, OR). Fetal bovine serum, RPMI 1640 medium and sodium pyruvate were obtained from Gibco/BRL (Grand Island, NY).

Culture of human thyroid papillary cancer cells

Human thyroid papillary cancer cell line, CG3, was kindly provided by Dr Lin. Its characterization had been described before.[15] CG3 cells were cultured in the RPMI medium supplemented with 10% fetal bovine serum and 100 mM sodium pyruvate in a humidified 5% CO_2 atmosphere at 37°C. The medium was changed every 2 days. Cells were seeded at the density of 10^6 cells/dish in 10-cm plastic culture dishes. After 2–3 days, the cells were subcultured using trypsin/EDTA at 70–90% subconfluence.

Cell counts

Cultured cells (3×10^4 cells/ml, 600 μl) in 24-well plates were harvested by trypsinization and then resuspended in RPMI medium. The number of living cells was counted with a hemocytometer after Trypan blue staining.

Cell viability assay

The method used was modified from Skehan *et al.*[16] Cultured cells (3×10^4 cells/ml, 100 μl) seeded in 96-well plates were washed with phosphate-buffered saline (PBS) and then fixed with 4% trichloroacetic acid (TCA) at 4°C for 1 h. Cells were washed with tap water 5 times and then stained with 0.4% sulforhodamine B (SRB) dissolved in 1% acetic acid for 10 min. At the end of staining the SRB solution was discarded, then the plates were rinsed with 1% acetic acid for 4 times. Bound dye was dissolved with 100 μl 20 mM Tris base buffer for 10 min in a gyratory shaker and then the absorbance at 570 nm was measured on a microplate reader.

Preparation of cell extracts

Treated cells were washed twice with PBS, scraped with a rubber policeman and resuspended in the lysis buffer (50 mM Tris, pH 7.5, 150 mM NaCl, 10 mM EDTA, 10% NP-40, 1 mM sodium vanadate, 0.5% sodium deoxycholate, 0.1% SDS, 1 mM PMSF, 10 μg/ml aprotinin and 10 μg/ml leupeptin). Cell lysates were clarified by centrifugation at 12 000 *g* for 10 min. An appropriate amount of protein was applied to measure the caspase activity.

Caspase activation

The method used to estimate the caspase activity was modified from Thornberry.[17] Caspase activity was assessed by the cleavage of site-selected tetrapeptide reporter substrates with the relative specificity of DEVD-AMC (caspases-3) and DQTD-AMC (caspase-7). Total lysates containing 40 μg of protein were pre-incubated at 30°C with assay buffer and then with 50 μM peptide substrates for 60 min. Fluorescence generated by the release of the fluorogenic group AMC (7-amino-4-methyl-coumarin) upon cleavage by caspases, was detected at the excitation wavelength of 360 nm and the emission wavelength of 460 nm with a microplate fluorescence reader (CytoFluor 2300). The signal strength representative of caspase activity was corrected for background and standardized to different amount of AMC.

Determination of ROS

Intracellular ROS were detected by flow cytometry using DCFH-DA as a probe.[18] DCFH-DA was applied to visualize and measure intracellular ROS production in the 15d-PGJ_2-treated CG3 cells with the use of flow cytometry. CG3 cells were treated with 15 μM 15d-PGJ_2 for the indicated periods and then incubated with 10 μM DCFH-DA for 30 min. At the end of incubation, cells were washed with PBS, detached by trypsinization, collected by centrifugation and suspended in PBS containing 5 μg/ml of PI for 10 min before flow cytometry. PI treatment of cell can differentiate between intact and damaged membrane of cells, since damaged cell membrane allows the entrance of this dye into the cells. For DCFH analysis, only PI^- cells were obtained. The intracellular ROS and the cell membrane integrity as indicated by the fluorescence of DCF and PI, respectively, were measured by a Becton Dickinson FACSCalibur flow

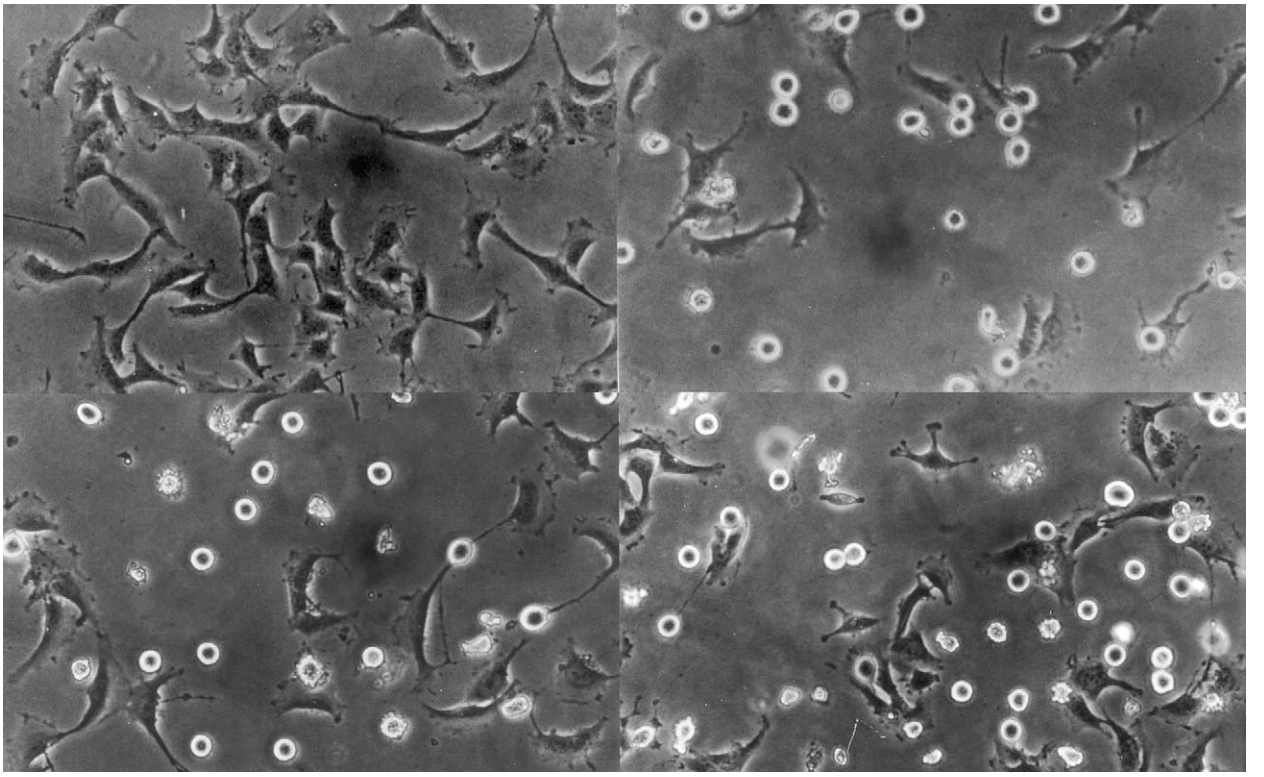

Figure 1. The morphological changes of CG3 cells during 15d-PGJ$_2$ incubation. Before incubation (left upper), and 12 (right upper), 24 (left lower) and 48 (right lower) h after incubation

cytometer at an excitation wavelength of 488 nm and an emission wavelength of 520 nm.

Estimation of intracellular chelatable iron

The method used to estimate the level of intracellular chelatable iron was modified from Epsztejn *et al.*[19] At the end of 15d-PGJ$_2$ incubation, CG3 cells were washed with PBS, detached by trypsinization, collected by centrifugation, and suspended in PBS containing 0.05 μM calcein-AM and 5 μg/ml PI for 5 min. The suspension was centrifuged, and then cells were washed with PBS and resuspended in a 10 mM HEPES buffer containing DTPA (2 mM). The calcein fluorescence of the cells was measured using a Becton Dickinson FACSCalibur flow cytometer at an excitation wavelength of 488 nm and an emission wavelength of 520 nm.

Results

15d-PGJ$_2$ induces apoptosis of cg3 cells

Figure 1 shows the morphologic changes of CG3 cell after incubation with 15d-PGJ$_2$ for up to 48 h.

The. cytotoxic effect of 15d-PGJ$_2$ was further investigated using Trypan blue exclusion assay. As shown in Figure 2(a), viability of CG3 cell decreased to 50% after treatment with 15 μM 15d-PGJ$_2$ for 24 h. As shown in Figure 2(b), the activity of caspase-3 and -7 increased after treatment with 15d-PGJ$_2$ for 12 h or more. The results indicate 15d-PGJ$_2$ induced apoptosis of CG3 cells.

15d-PGJ$_2$ induces intracellular peroxides generation

The effect of 15d-PGJ$_2$ on the generation of intracellular ROS was investigated using the oxidant-sensitive biological probe, DCFH-DA. As shown in Figure 3, the fluorescence intensity of DCFH-DA increased after treatment with 15d-PGJ$_2$ and reached a plateau in 1 h. The results indicated 15d-PGJ$_2$ induces intracellular peroxides generation.

Iron mediates 15d-PGJ$_2$-induced oxidative stress

Various functional and enzyme inhibitors were employed to detect whether these agents can reduce 15d-PGJ$_2$-induced ROS generation. After CG3 cells

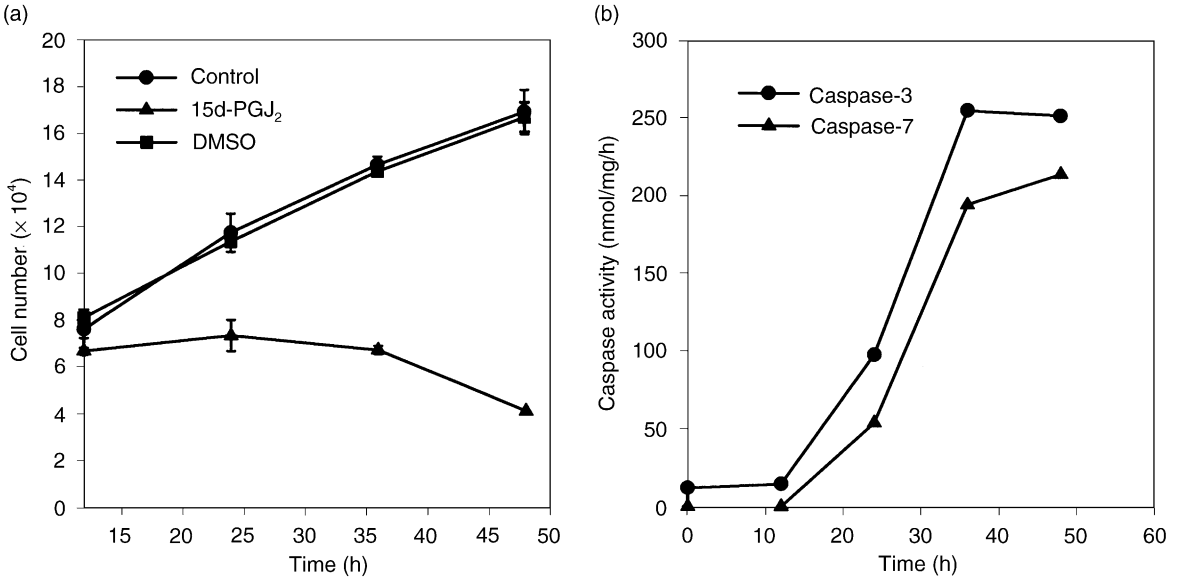

Figure 2. (a) Cytotoxic effect of 15d-PGJ_2 on CG3 cells. CG3 cells were incubated with 15 μM 15d-PGJ_2 from 12 to 48 h. Trypan blue dye exclusion assay was performed to measure the number of viable cells as described in Materials and methods. (b) Effect of 15d-PGJ_2 on the caspase activities of CG3 cells. The activities of caspase-3 and -7 were assessed after incubation with 15 μM 15d-PGJ_2 for different durations.

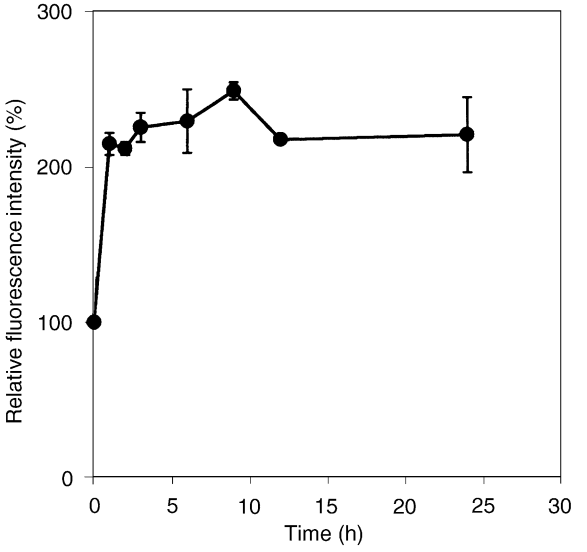

Figure 3. Effect of 15d-PGJ_2 on the generation of reactive oxygen species in CG3 cells. CG3 cells were treated with 15 μM 15d-PGJ_2 for 1, 2, 3, 6, 9, 12 and 24 h. Generation of ROS was determined by DCFH-DA assay.

were incubated with inhibitors for 1 h, 15 μM 15d-PGJ_2 was added for an additional 3 h of incubation. As shown in Figure 4, pretreatment with mitochondrial oxidative phosphorylation inhibitors including CCCP (100 μM), Oli (5 μM), Cys A (1 μg/ml) and Rot (5 μM) did not prevent 15d-PGJ_2-induced oxidative stress. NADPH oxidase inhibitor DPI (20 μM), xanthine oxidase inhibitor All (400 μM), as well as NO synthase inhibitor L-NMMA (1 μg/ml) could not reduce the 15d-PGJ_2 -induced generation of ROS, either. However, the iron chelator DFO (50 μM) eliminated 15d-PGJ_2-induced ROS generation as effectively as the ROS scavenger NAC (5 mM) and Cat (500 U/ml). These results suggested that iron ions mediate 15d-PGJ_2-induced oxidative stress.

Correlation between ROS generation and cytotoxicity

To assure that the generation of ROS was the cause of 15d-PGJ_2-induced apoptosis, we examined the cell viability with the SRB assay, whereby CG3 cells were co-incubated with 15d-PGJ_2 and compounds mentioned above. As shown in Figure 5, NAC (5 mM), DFO (50 μM) and Cat (500 U/ml) effectively block the cytotoxic effect of 15d-PGJ_2. These results indicate that oxidative stress induced by 15d-PGJ_2 caused the apoptosis of CG3 cells.

15d-PGJ_2 increases intracellular chelatable iron ions

The level of intracellular chelatable iron in 15d-PGJ_2-treated CG3 cells was estimated using the probe calcein-AM to clarify whether intracellular chelatable

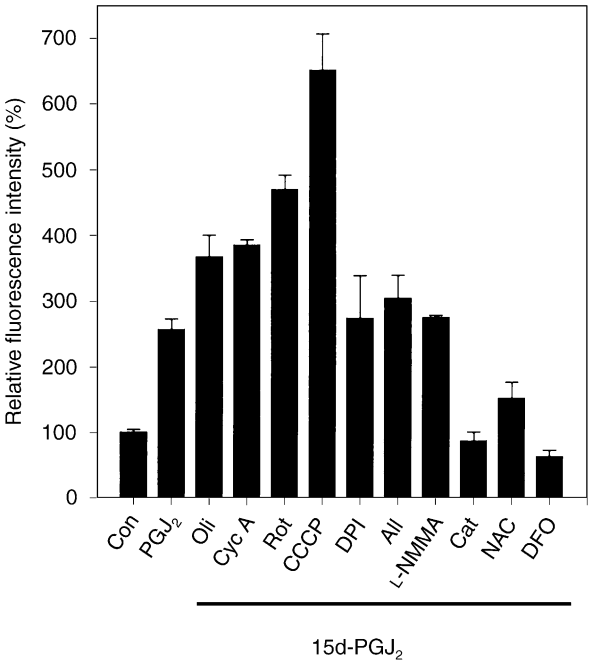

Figure 4. Effects of various compounds on the generation of reactive oxygen species in 15d-PGJ$_2$-treated CG3 cells. CG3 cells were treated with mitochondrial oxidative phosphorylation inhibitors including 100 μM CCCP, 1 μg/ml Cys A, 5 μM Oli and 5 μM Rot. CG3 cells were pretreated with ROS synthesis inhibitors including 20 μM DPI, 400 μM All and 1 μg/ml L-NMMA or free radical scavengers: 500 U/ml Cat, 5 mM NAC and 50 μM DFO. The results were based on three different experiments, each based on three repeats. These results were representative of a series of three similar experiments.

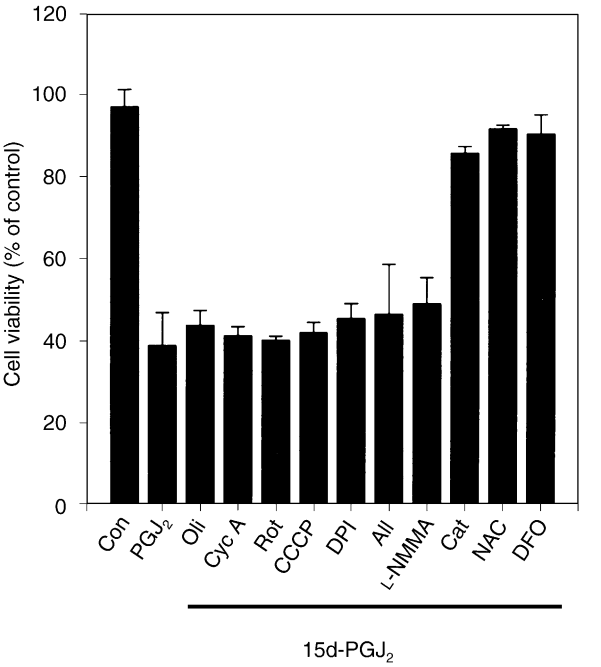

Figure 5. The protective effects of various compounds on 15d-PGJ$_2$-induced cytotoxicity. CG3 cells were pretreated with mitochondrial oxidative phosphorylation inhibitors, xanthine oxidase inhibitors, antioxidant enzymes, antioxidants and DFO. The cytotoxicity was measured by the SRB method over 48 h and the number of events was expressed as a percentage of control. The results were based on three different experiments, each based on three repeats.

iron is involved in 15d-PGJ$_2$-induced oxidative stress. This method is based on the fact that total calcein fluorescence is quenched by bound iron. As shown in Figure 6, the calcein-AM fluorescence increased in CG3 cells after treatment with 15d-PGJ$_2$ for 3–12 h. This suggests there is an increase of intracellular chelatable iron ions after treatment with 15d-PGJ$_2$ in CG3 cells.

Discussion

In this study, 15d-PGJ$_2$ treatment resulted in decreasing cell numbers and increasing caspase (caspase-3 and -7) activities of CG3 cells. Apoptosis of CG3 cells was also proved by morphological observation. Recently, Ohta *et al.* reported that ligands for PPAR-γ inhibit growth and induce apoptosis of human papillary thyroid carcinoma cells.[6] An increase of c-*myc* mRNA but no change of *bcl-2* or *bax* expression

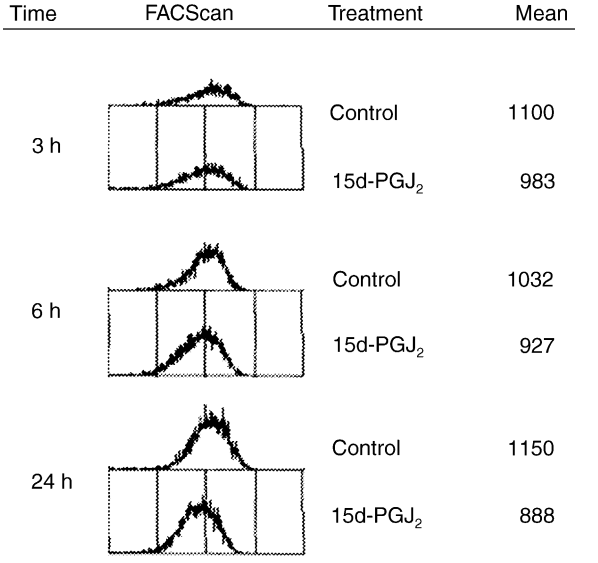

Figure 6. The change of intracellular free iron in CG3 cells during 15d-PGJ$_2$ treatment. CG3 cells were treated with 15 μM 15d-PGJ$_2$ for 3, 6 and 24 h. The fluorescent excitation value was expressed as mean value.

was noted.[6] The apoptosis of CG3 cells could be prevented by pretreatment with the free radical scavenger NAC and catalase. This suggests that 15d-PGJ_2-induced apoptosis of CG3 cells was through generation of oxidative stress. Intracellular ROS production by 15d-PGJ_2 treatment in CG3 cells was also demonstrated. There are many potential cellular sources of ROS generation, including cytosolic xanthine oxidase, membrane NADPH oxidase and the mitochondrial electron transport system. However, various inhibitors of these enzymes were unable to block the apoptosis induced by 15d-PGJ_2. It was interesting that the iron chelator DFO completely eliminated 15d-PGJ_2-induced ROS generation and cytotoxicity in CG3 cells. These results indicated that iron could mediate 15d-PGJ_2-induced oxidative stress in CG3 cells. Previous study had shown that 15d-PGJ_2 was a potential inducer of oxidative stress in human neuroblastoma SH-5Y5Y cells and that mitochondria were the source of the induced ROS;[7] this differed from the result of this study. We believe that the variance could be due to the different expression systems of these cell lines.

Iron is the most abundant transition metal ion in most terrestrial organisms, and is essential for cellular metabolism and growth. In normal tissue, iron rarely exists as a free ion but rather is bound to a variety of proteins. Many enzymes (catalases and oxidases) and proteins (hemoglobin and myoglobin) contain iron, which allows electron shuttling or oxygen binding and transport. However, there is a free iron pool that is chelatable by DFO. The small transit pool of chelatable iron is thought to catalyze the generation of the ROS.[20,21] These studies suggest that an increase in the cellular chelatable iron pool plays the key role in the pathogenesis of various free radical-mediated cell injuries, which result in neurodegenerative disorders and cardiovasular disease.[22,23] In our present study, we demonstrated that 15d-PGJ_2 increased intracellular chelatable iron, leading to ROS generation and apoptosis in CG3 cells. The ROS generation reached a plateau in 60 min in this study. A previous study indicated that UV radiation caused an immediate release of chelatable iron via proteolysis of ferritin in human skin fibroblast cells.[24] It was reported that higher expression of transferrin receptors could result in accumulation of iron.[25] It is possible that the increase of free iron by 15d-PGJ_2 is by the same mechanisms. This still has to be further confirmed. In our study, we measured mitochondrial transmembrane potential by flow cytometry using Rodamine 123 as a probe, and collected the data in short-term (1 h) and long-term (12–36 h) studies. The results revealed that there was no difference between treated and non-treated cells (data not shown here). If the ROS (or chelatable iron) increase is due to electrons leaking from the electron transport chain, we could detect a decrease of mitochondrial transmembrane potential. This suggests that the iron of heme or non-heme protein in the electron transport chain was not the source of intracellular chelatable iron. Many studies have indicated that 15d-PGJ_2-induced apoptosis is accompanied with PPAR-γ activation,[26] but the mechanism by which PPAR-γ ligands induce apoptosis remains unknown. We believe that the PPAR-γ-activating pathway may be involved in 15d-PGJ_2-induced oxidative stress, which needs to be further studied.

Conclusion

In conclusion, 15d-PGJ_2 induces an increase of intracellular iron and leads to the generation of ROS in a thyroid papillary cancer cell line, CG3. Then, intracellular ROS induces apoptosis of CG3 cells. Our observation may have useful implications for devising potential therapeutic strategies for human thyroid papillary carcinoma.

Acknowledgments

We thank Dr Jen-Der Lin in Chang Gung Memorial Hospital for the supply for the thyroid cancer cell line.

References

1. Kliewer SA, Umesono K, Noonan DJ, Heyman RA, Evans RM. Convergence of 9-*cis* retinoic acid and peroxisome proliferator signalling pathways through heterodimer formation of their receptors. *Nature* 1992; **358**: 771–4.
2. Kilgore MW, Tate PL, Rai S, Sengoku E, Price TM. MCF-7 and T47D human breast cancer cells contain a functional peroxisomal response. *Mol Cell Endocrinol* 1997; **129**: 229–35.
3. Tsubouchi Y, Sano H, Kawahito Y, *et al.* Inhibition of human lung cancer cell growth by the peroxisome proliferator-activated receptor-gamma agonists through induction of apoptosis. *Biochem Biophys Res Commun* 2000; **270**: 400–5.
4. Sato H, Ishihara S, Kawashima K, *et al.* Expression of peroxisome proliferator-activated receptor (PPAR)gamma in gastric cancer and inhibitory effects of PPARgamma agonists. *Br J Cancer* 2000; **83**: 1394–400.

5. Butler R, Mitchell S H, Tindall DJ, Young CY. Nonapoptotic cell death associated with S-phase arrest of prostate cancer cells via the peroxisome proliferator-activated receptor gamma ligand, 15-deoxy-delta12,14-prostaglandin J2. *Cell Growth Different* 2000; **11**: 49–61.
6. Ohta K, Endo T, Haraguchi K, Hershman JM, Onaya T. Ligands for peroxisome proliferator-activated receptor gamma inhibit growth and induce apoptosis of human papillary thyroid carcinoma cells. *J Clin Endocrinol Metab* 2001; **86**: 2170–7.
7. Kondo M, Oya-Ito T, Kumagai T, Osawa T, Uchida K. Cyclopentenone prostaglandins as potential inducers of intracellular oxidative stress. *J Biol Chem* 2001; **276**: 12076–83.
8. Chance B, Sies H, Boveris A. Hydroperoxide metabolism in mammalian organs. *Physiol Rev* 1979; **59**: 527–605.
9. Nikjoo H, O'Neill P, Terrissol M, Goodhead DT. Modelling of radiation-induced DNA damage: the early physical and chemical event. *Int J Radiat Biol* 1994; **66**: 453–7.
10. Klein G. The approaching era of the tumor suppressor genes. *Science* 1987; **238**: 1539–45.
11. Gamaley IA, Klyubin IV. Roles of reactive oxygen species: signaling and regulation of cellular functions. *Int Rev Cytol* 1999; **188**: 203–55.
12. Nakamura H, Nakamura K, Yodoi J. Redox regulation of cellular activation. *Annu Rev Immunol* 1997; **15**: 351–69.
13. Kasahara Y, Iwai K, Yachie A, *et al.* Involvement of reactive oxygen intermediates in spontaneous and CD95 (Fas/APO-1)-mediated apoptosis of neutrophils. *Blood* 1997; **89**: 1748–53.
14. Watson RW, Rotstein OD, Jimenez M, Parodo J, Marshall JC. Augmented intracellular glutathione inhibits Fas-triggered apoptosis of activated human neutrophils. *Blood* 1997; **89**: 4175–81.
15. Lin JD, Chao TC, Weng HF, Huang HS, Ho YS. Establishment of xenografts and cell lines from well differentiated human thyroid carcinoma. *J Surg Oncol* 1996; **63**: 112–8.
16. Skehan P, Storeng R, Scudiero D, *et al.* New colorimetric cytotoxicity assay for anticancer-drug screening. *J Natl Cancer Inst* 1990; **82**: 1107–12.
17. Thornberry NA. Interleukin-1 beta converting enzyme. *Method Enzymol* 1994; **244**: 615–31.
18. Bass DA, Parce JW, DeChatelet LR, Szejda P, Seed MC, Thomas M. Flow cytometric studies of oxidative product formation by neutrophils: a graded response to membrane stimulation. *J Immunol* 1983; **130**: 1910–7.
19. Epsztejn S, Khlon O, Glickstein H, Breuer W, Cabantchik I. Fluorescence analysis of the labile iron pool of mammalian cells. *Anal Biochem* 1997; **248**: 31–40.
20. Ryan TP, Aust SD. The role of iron in oxygen-mediated toxicities. *Crit Rev Toxicol* 1992; **22**: 119–41.
21. Rothman RJ, Serroni A, Farber JL. Cellular pool of transient ferric iron, chelatable by deferoxamine and distinct from ferritin, that is involved in oxidative cell injury. *Mol Pharmacol* 1992; **42**: 703–10.
22. Lee FY, Lee TS, Pan CC, Huang AL, Chau LY. Colocalization of iron and ceroid in human atherosclerotic lesions. *Atherosclerosis* 1998; **138**: 281–8.
23. Qian ZM, Wang Q. Expression of iron transport proteins and excessive iron accumulation in the brain in neurodegenerative disorders. *Brain Res* 1998; **27**: 257–67.
24. Pourzand C, Watkin RD, Brown JE, Tyrrell RM. Ultraviolet A radiation induces immediate release of iron in human primary skin fibroblasts: the role of ferritin. *Proc Natl Acad Sci USA* 1999; **96**: 6751–6.
25. Verrijt CE, Kroos MJ, Huijskes-Heins MI, *et al.* Accumulation and release of iron in polarly and non-polarly cultured trophoblast cells isolated from human term placentas. *Eur J Obstet Gynecol R B* 1999; **86**: 73–81.
26. Chinetti G, Griglio S, Antonucci M, *et al.* Activation of proliferator-activated receptors alpha and gamma induces apoptosis of human monocyte-derived macrophages. *J Biol Chem* 1998; **273**: 25573–80.

(Received 20 March 2002; revised form accepted 14 May 2002)